Enhancing Lung Cancer Diagnosis through CT Scan Image Analysis using Mask-EffNet

Sachikanta Dash[1] ,Sasmita Padhy[2,*], Preetam Suman[3], Rajendra Kumar Das[4]

[1,]Computer Science and Engineering , GIET University, Gunupur, Odisha, India
[2,3]School of Computing Science and Engineering, VIT Bhopal University, Kothrikalan, Sehore, MP, India,
[4]Computer Science and Engineering , KIIT Deemed to be University, BBSR, Odisha, India

*Corresponding Email : pinky.sasmita@gmail.com

Received May 12, 2024, Revised July 12, 2024, Accepted July 17, 2024, Published December 19, 2024

Abstract. *CT scans efficiently detect lung cancer. A good prediction method is crucial. Recently, deep convolutional neural networks (CNN) have influenced picture categorization algorithms. This article presents a hybrid strategy using an upgraded deep transfer learning EfficientNet and a masked autoencoder for image-based distribution estimation (MADE). MADE improves feature acquisition, dimensionality, uncertainty, imbalanced data, transfer learning, and model interpretability before lung cancer categorization. These benefits improve classification accuracy and data use. Mask-EffNet, the proposed model, has two phases. The initial phase uses MADE to extract features. Using a pre-trained EfficientNet model, types are classified next. Mask-EffNet is tested using EfficientNetB7. The study uses the "IQ-OTH/NCCD" benchmark dataset, which includes lung cancer patients classified as benign, malignant, or normal. Mask-EffNet has 98.98% test set accuracy with ROC scores of 0.9782–0.9872. We tested the suggested pre-trained Mask-EffNet against different CNN architectures. The EfficientNetB7-based Mask-EffNet outperforms various CNNs in accuracy and efficacy, as expected.*

Keywords:
Auto encoder, CT scan image, lung cancer, EfficientNet, CNN

1. Introduction

According to the World Health Organization [1], cancer is ranked as the second most common cause of death worldwide. In the United States, lung cancer is the leading cause of death, claiming 1.8 million lives each year. Timely identification with Lung Cancer Detection (LCD) is crucial for personalized therapies and prognosis. Artificial intelligence assists in surmounting healthcare obstacles, diminishing the time required for diagnosis, and augmenting the quality of healthcare [2,3]. This study explores the application of artificial intelligence (AI) in aiding conventional lung cancer screening through the use of biomedical imaging techniques, as opposed to innovative breath analysis methods [4,5]. Researchers are researching computer ways to automate the process of lung cancer categorization and minimize the inherent bias and uncertainty in traditional visual analysis. This advancement enhances the precision of lung cancer therapies for different types of the illness. This enhances the dependability and accuracy of determining the stage and type of cancer, while also providing comprehensive information for patient care [6]. The recent breakthroughs in artificial intelligence have greatly benefited the development of automated systems that effectively process medical imaging data, particularly in the accurate classification of lung cancer. Furthermore, these strategies have the potential to enhance the overall efficiency of lung cancer categorization, while also yielding more unbiased and accurate outcomes [7, 8].

Traditional diagnostic methods, such as MRI and CT scans, are essential in the diagnosis of lung cancer. CT scans are highly efficient in identifying abnormalities, such as cancer, in the chest, by utilizing X-rays. Machine learning, specifically Convolutional Neural Networks (CNNs), assist in visual analysis, albeit a substantial amount of data is necessary for their effectiveness [9]. Despite challenges in obtaining datasets, deep learning models demonstrate promise in accurate cancer classification, offering the potential to enhance existing diagnostic techniques and reduce human error.

By augmenting the existing trained models with new datasets, transfer learning (TL) effectively addresses the limitations of CNNs. Certain techniques involve augmenting pre-existing layers or constructing novel ones to enable end-to-end training [10]. Katsamenis et al. (2020) conducted an investigation on the utilization of TL for the identification of COVID-19 pneumonia using X-rays. Transfer Learning (TL) offers a reliable approach to enhance the performance of models and adapt them to various medical imaging tasks [11].

Regarding healthcare image analysis, the use of EfficientNets in TL offers the ability to reduce certain frequent restrictions. EfficientNets are renowned for their ability to efficiently extract pertinent and representative features from photos. EfficientNetB7 models, which have undergone pretraining on extensive datasets like as ImageNet, offer superior accuracy and robustness in the classification of lung cancer through the application of transfer learning [12]. Our method offers superior computational efficiency

compared to existing deep learning architectures, enabling speedy and accurate interpretation of medical pictures for the detection of lung cancer [13]. This enhancement to the categorization process is anticipated to enhance the effectiveness and efficiency of medical picture analysis.
The primary objective of this study is to categorize lung nodules on CT scans as benign, malignant, or normal based on the identification of cancerous cells. In order to achieve this categorization, the proposed model, Mask-EffNet, employs a two-step process. The first phase is extracting features using the MADE algorithm, while the second step involves categorizing different classes using a pre-trained EfficientNetB7 model. The performance of Mask-EffNet is assessed using several pre-trained models.

The following are the primary contributions of this article:

- Using MADE and EfficientNetB7, we created a unique masked transfer learning method called Mask-EffNet for lung cancer categorization.
- To overcome the skewness of the data, we used the augmentation method to solve the severe imbalance problem.
- To extract features, we employed a Masked Autoencoder for The Distribution Estimation (MADE).
- To highlight Mask-EffNet's superiority over other classification models, we compared it for assessing methods by execution time, computational complexity reveals feasibility.
- When compared to existing approaches, our suggested model Mask-EffNet outperforms them and identifies lung cancer from CT scan pictures.

The paper's remaining sections are arranged in the following manner. Section II describes various literatures, while Section III describes the proposed algorithm. Conclusion and discussion of Section IV on performance metrics are presented in Section V. Section VI contains a comparative analysis, and Section VII will have an outline of future work after the paper is concluded.

2. Literature Study

Integrating deep learning (DL) and transfer learning (TL) in survival models for lung cancer is crucial for adapting to real-world populations' diverse characteristics. Many approach optimizes model performance across different domains, addressing variations in variables and enhancing prediction accuracy for improved patient outcomes. Few of them are analyzed below.

The article by Raza et al. [14] presents Lung-EffNet, a lung cancer classification predictor that utilises transfer learning. Lung-EffNet is developed from the EfficientNet architecture and is boosted with additional top layers for improved classification. Lung-EffNet achieves 99.10% accuracy on IQ-OTH/NCCD dataset, showcasing high ROC scores. Lung-EffNet outperforms in terms of accuracy, efficiency, and scalability, compare to other models in a clinical setting.

Huseiny et al. [15] suggests a method for identifying cancerous nodules in CT scans of the lungs by employing deep neural networks (NN). Images are normalised and lung areas are isolated using basic pre-processing. Then, a modified GoogLeNet is fed into it using transfer learning. The system achieves an unprecedented 94.38% accuracy when training on the IQ-OTH/NCCD lung cancer dataset, outperforming prior benchmarks. An example of the usefulness of Deep NNs in medical image processing, this technique improves nodule diagnosis in CT images of the lungs.

Dubey et al. [16] investigates how well deep TL and ensemble deep learning (EDL) work for lung segmentation and COVID-19 classification. Data for the study came from a wide variety of Croatian and Italian healthcare facilities. Based on the premise that EDL is superior, it tests 12,000 CT slices. Comparing the EDL and TL models using fresh, undiscovered data shows that the EDL model obtains better accuracy. The notion is bolstered by this discovery. By proving EDL's efficacy on balanced and enhanced datasets, the statistical tests validate its reliability and stability. Both the visible and invisible perspectives are supported by these findings.

A DL system for lung cancer prediction using EfficientNetB3, ResNet50, and ResNet101 with TL is presented by Jassim et al. [17]. Their research looks at how well these models can detect lung cancer. Data augmentation guards against overfitting when trained on a dataset consisting of one thousand CT lung pictures divided into four categories. Performance is improved by score-level fusion and ensemble learning, outperforming current approaches with an accuracy of 99.44%. High accuracy and resilience in lung cancer prediction are demonstrated in the study, which underlines the efficiency of ensemble TL with diverse models. Wu et al. [18] presented STLF-VA, a self-supervised TL framework that uses visual attention and entire nodule volumes as features to improve nodule categorization. By methodically using 3D unlabeled CT images, it reduces the requirement for labelled samples. Strengthening interference resistance is the multi-view aggregative attention module's job. Performance on the CQUCH-LND and LIDC-IDRI datasets is higher than that of traditional models, according to the evaluation. Clinical chest CT scan analysis can be greatly improved with the help of this paradigm, which offers substantial advancements in nodule malignancy prediction.

The BERTL-HIALCCD method for efficient identification of lung and colon cancer (LCC) in histopathological images is introduced in the publication of AlGhamdi et al. [19]. The approach combines computer vision with transfer learning, using a deep convolutional recurrent neural network (DCRNN) for recognition and an improved ShuffleNet for feature

extraction. Parameters of DCRNN are fine-tuned by coati optimisation. Results from experiments conducted on a large dataset confirm the effectiveness of BERTL-HIALCCD as a cancer detection model.

For the purpose of classifying CT images of the lung as cancer, Saleh et al. [20] provide a CNN that combines TL and random forest. It builds the algorithm, compares its effectiveness, and preprocesses the data. The results prove that machine learning is the best tool for healthcare, especially for identifying and categorizing diseases. The outcomes demonstrate the promise of cutting-edge methods in enhancing diagnostic precision and healthcare delivery when contrasted with traditional CNNs devoid of transfer learning.

In their research, Mammeri et al. [21] suggest a way to use the LIDR-IDRI dataset to identify and categorise lung nodules. Bounding boxes are drawn around nodules using YOLO v7 for object identification. This helps radiologists trace them across CT slices. We compare different input images and find whole images yield the best detection results. For classification, we employ transfer learning with VGG16, achieving good performance in classifying nodules into benign, suspect, and malignant categories based on radiologists' assessments of malignancy. This approach shows promise in enhancing nodule classification accuracy and improving lung cancer diagnostics.

CT scans are vital for diagnosing lung cancer, with AI systems using transfer-learning models showing promise in improving precision and speed. TL adapts pre-existing models, aiding medical data analysis. The study by Shouka et al. [22] examines CNN based TL with RESNET, MobileNetV2, Xception, and VGG16, with ResNet yielding the highest testing accuracy at 0.94 and a testing loss of 0.16. This highlights potential enhancements in healthcare AI accuracy and efficiency.

A novel framework proposed by Sharma et al. [23] utilizes a customized Densenet-201 model for precise multi-class lung cancer categorization, employing TL and a residual structure. Experiments on the LCS25000 dataset showcase its remarkable 95% accuracy on the test set, demonstrating its ability to classify lung cancer types accurately. It also generalizes well to the TCGA lung cancer dataset, promising improved diagnostic abilities and patient care in pulmonary pathology.

Fu et al. [24] crafted a 3D deep transfer learning model, differentiating between IAC and MIA using CT images of GGNs. MedicalNet pre-training and a fusion model facilitated classification, employing TL for predictive modeling, validated internally and externally across three centers. With 999 lung GGN images, the model achieved high diagnostic efficacy, with accuracies ranging from 78% to 89% and AUCs from 82% to 95%, demonstrating its robustness and potential clinical utility.

Ren et al. [25] introduce LCGANT, a hybrid framework comprising LCGAN for generating synthetic lung cancer images and VGG-DF for classification. Achieving 99.84% accuracy, precision, sensitivity, and F1-score, it surpasses other methods in lung cancer classification. LCGANT resolves overfitting, demonstrating superior performance and promising advancements in lung cancer diagnostic accuracy.

This study by Lague et al. [26] aimed to predict PET results from contrast-enhanced CT scans using various feature extraction methods. Machine learning models were trained on data from 100 lung cancer patients, incorporating traditional radiomics features, deep features from EfficientNet-CNN, and a hybrid approach. The random forest model combining both approaches have achieved the good performance results, with an AUC of 0.871 and SBS of 35.8%. This demonstrates the complementary nature of traditional and deep radiomics features for non-invasive N-staging in lung cancer, enhancing diagnostic accuracy.

Atiya et al. [27] introduce a dual-state transfer learning method employing deep CNNs to enhance lung cancer classification from CT scans. By leveraging pre-trained models like DCNN, VGG16, Inceptionv3, and RestNet50, the proposed model achieves 94% training accuracy, with 92.57% validation and 96.12% testing accuracy. Outperforming existing models, this approach enhances lung cancer screening precision and effectiveness, showcasing the potential of dual-state transfer learning and deep CNNs in medical image analysis.

In order to diagnose lung cancer, Humayun et al. [28] proposed an approach that uses a CAD system with a deep neural network and strong DL algorithms. Data augmentation, categorization with pre-trained CNN models, and localization make up the procedure. A method for dealing with data scarcity, TL generates a diagnostic tool with fewer parameters and less invasiveness than the state-of-the-art models. At the 20th epoch, VGG 16 achieves an accuracy of 98.83% according to the performance metrics, which evaluate the architecture. Integrating with interfaces becomes easier and faster after preprocessing increases the model's reliability and prediction capacity. This study demonstrates how well TL techniques and models perform in medical picture evaluation when the dataset size is large.

For the purpose of lung cancer detection, Chui et al. [29] provide the MTL-MGAN method. While MGAN provides more training data and fills in domain gaps, this method focuses on making the most of transferability across source and target domains, making the model more adaptable and effective across different datasets and clinical contexts. There is a considerable improvement in accuracy compared to related efforts, according to evaluation on 10 datasets. Component effectiveness has been validated using ablation studies, which emphasize the feasibility of MTL and the bridging potential of MGAN.

This study by Saikia et al. [30] categorises lung nodules based on CT scan pictures into four distinct types: the includes the types of carcinomas like small-cell carcinoma, squamous-cell carcinoma, adenocarcinoma, , and large-cell carcinoma. The suggested hybrid methodology combines VGG networks with support vector machine and random forest, leading to a decrease in computational complexity. The hybrid algorithms surpass current techniques for classifying lung nodules in CT scans, with an accuracy of 98.70%.

The research by Nigudgi et al. [31] presents a method for classifying lung CT images and detecting cancer using transfer learning. A composite model combining the features of AlexNet, VGG, and GoogleNet is utilised to extract features, which are then classed using a multi-class SVM. Model trained on IQ-OTH/NCCD set, achieving 97% accuracy, outperforming others. Dataset split for training and validation. Real-time transfer learning for CT lung slice classification. The procedure entails performing pre-processing and segmentation through the use of K-means clustering. Additionally, it requires fine-tuning the weighted VGG deep network and deploying it using Nvidia tensor-RT for real-time applications. The suggested model, which was trained on 19,419 CT slices, demonstrates enhanced classification metrics with statistical validation.

The paper by Dadgar et al. [32] presents a hybrid convolutional deep transfer learning model that combines different architectures, including VGG16, ResNet152V2, MobileNetV3. Various model architectures were constructed and compared after adjusting their hyperparameters. The top-performing model, InceptionResNetV2 with transfer learning, achieved an accuracy of 91.1%, precision of 84.9%, AUC of 95.8%, and F1-score of 81.5% in classifying lung tumours using 1000 pre-processed CT scans.

Mammeri et al. [33] utilized data from 601,480 lung cancer patients from SEER and 4,512 from GYFY. Their primary model trained on SEER was internally validated, externally validated with GYFY through transfer learning. Model performance was evaluated using C-indexes and explored in handling missing data and AI prediction certainty. In the SEER training dataset, DeepSurv outperformed the Cox model with C-indexes of 0.792 and 0.714, respectively. Testing on GYFY, DeepSurv yielded C-indexes of 0.727, surpassing the Cox model's 0.692. DeepSurv exhibited high AI certainty and improved prediction accuracy with transfer learning and missing data handling.

This study by Wang et al. [34] presents a new residual neural network that can accurately classify different forms of lung cancer based on CT data. In order to deal with the lack of data, a method called medical-to-medical transfer learning is being investigated. This involves initially training on the luna16 dataset and then refining the model on a private dataset from Shandong Provincial Hospital. The method achieves an accuracy of 85.71%, which is higher than models trained with 2054 labels. It outperforms AlexNet, VGG16, and DenseNet, making it an efficient and non-invasive tool for disease diagnosis. Table 1 provides a brief comparison of existing work with the proposed work.

Table 1 Current state of the art model on lung cancer detection

Author	Model	Methodology	dataset	Remarks
Raza et al. [14]	Lung-EffNet	Lung-EffNet achieves 99.10% accuracy on lung cancer diagnosis.	IQ-OTH/NCCD	Accuracy of 98.10% and demonstrates high ROC scores
Huseiny et al. [3]	modified GoogLeNet	Pre-processed lung images fed into modified GoogLeNet DNN achieve 94.38% accuracy in nodule detection, surpassing benchmarks.	IQ-OTH/NCCD	achieves 94.38% accuracy
Jassim et al. [16]	EfficientNetB3, ResNet50, and ResNet101	A deep-learning system achieves 99.44% accuracy in lung cancer prediction, employing transfer learning and ensemble methods.	1000 CT lung images	achieving 98.44% accuracy
Wu et al. [17]	self-supervised transfer learning framework	Utilizes 3D CT images, enhancing nodule malignancy prediction accuracy	CQUCH-LND and LIDC-IDRI datasets	Enhances nodule malignancy prediction with 3D CT
Mammeri et al. [20]	Utilizing YOLO v7 for object detection, VGG16	YOLO v7 detects lung nodules, aiding radiologists, while VGG16 classifies them accurately	LIDR-IDRI	Good nodule classification performance attained
Shouka et al. [21]	RESNET, MobileNetV2, Xception, and VGG16	AI using transfer-learning improves lung cancer diagnosis accuracy and efficiency in CT scans	IQ-OTH/NCCD	accuracy at 0.94 and a testing loss of 0.16
Sharma et al. [22]	customized Densenet-201	Customized Densenet-201 achieves 95% accuracy in lung cancer classification.	LCS25000, TCGA lung cancer dataset	95% accuracy
Proposed Mask-EffNet	Mask-EffNet	EfficientNetB7 with Masked autoencoder	IQ-OTH/NCCD	98.98% accuracy

3. Materials and Methods

The following section describes the dataset and approach used to train the suggested algorithm for multi-class lung cancer categorization from CT scans. Fig. 1 depicts the general process of the suggested methodology. It begins by loading CT scan slices, which then undergo several pre-processing steps. Given the challenge of acquiring annotated medical imaging data, data augmentation artificially boosts the training instances. This approach leverages transfer learning, tailored for lung cancer classification (benign, malignant, and normal). Following an introduction, subsequent sections delve into pre-processing, data augmentation, and specifics of the suggested model. This comprehensive approach tackles the intricate challenges of medical image analysis and classification effectively.

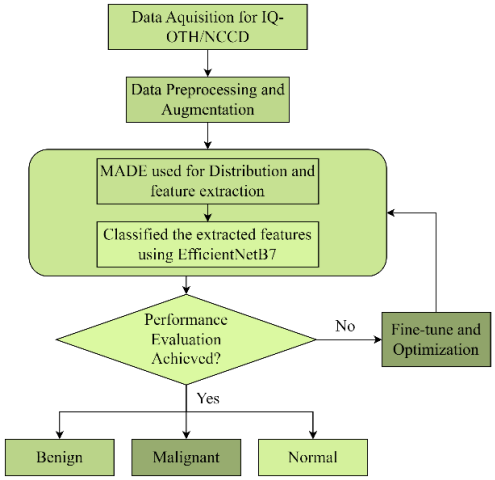

Fig. 1. Flow diagram of the Proposed work

A. Description of the Dataset

The IQ-OTH/NCCD dataset is ideal for lung cancer research due to its high-quality, diverse imaging data, and extensive expert annotations, ensuring reliable and accurate models. It includes comprehensive metadata, such as patient demographics and clinical history, enhancing study depth. Publicly accessible, it allows for reproducible and comparable studies. The balanced class distribution and sophisticated imaging modalities like CT and PET scans strengthen model practicality. Its robust community support and impressive features make it a reliable basis for precise and applicable machine learning models.

The studies are carried relying on lung cancer dataset "Iraq-Oncology Teaching Hospital/National Center for Cancer Diseases (IQ-OTH/NCCD)" (Alyasriy et al. [12]). It was gathered for over three months from them in 2019. Fig. 2 represents sample Images from IQ-OTH/NCCD dataset. The dataset comprises CT scans from individuals with varying lung health statuses, annotated by oncologists and radiologists. It includes 1142 chest CT scan images from 126 patients, reflecting diverse demographics. Cases were classified into benign, malignant, or normal categories (Fig. 2), with 42 malignant, 20 benign, and 64 normal cases examined. Originally in DICOM format with 224 x 224 resolution, later, scans were converted to JPEG format for easier accessibility. The collected dataset, accessible through Kaggle, provides valuable insights into lung cancer classification. Table 2 class wise categorization of collected dataset facilitating researcher to do research and analysis in the field of medical imaging, thereby advancing our understanding of lung cancer detection and diagnosis.

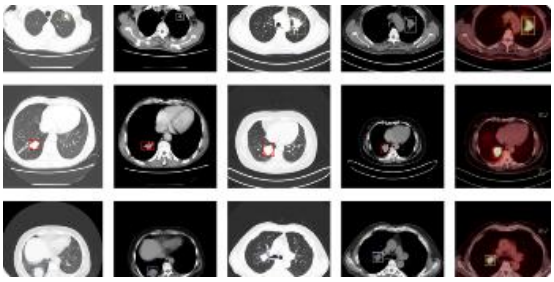

Fig. 2. Sample Images from IQ-OTH/NCCD dataset.

Table 2 IQ-OTH/NCCD Dataset of different classes

Type	No. of Patients	No. of Samples
Class of Benign	20	122
Class of Malignant	42	564
Normal Class	64	456
All Total	126	1142

B. Data Pre-processing

This section describes over the pre-processing steps that were performed on the raw data prior to model training and testing. Every image in every group are initially shuffled for impartial training before being split into an 80:20 train-test ratio, with 80% of the amount of images examined into train set for training operation and 20% samples used for test set for the model assessment on undiscovered test instances. Table 3 summarizes the dataset's class-wise distribution following the train and test split. Undesirable elements like background and noise in original CT scan images could disrupt training. To mitigate this, the largest lung contour's peak points were extracted, eliminating unwanted regions. This process, depicted in Fig. 3, ensures cleaner data for more effective model training.

Table 3 Training and Testing split-up of 80:20 ratio

Type of Class	Split-up	# Sample	Total
Benign	Training	97	897
Malignant		450	
Normal		360	
Benign	Testing	25	235
Malignant		114	
Normal		96	

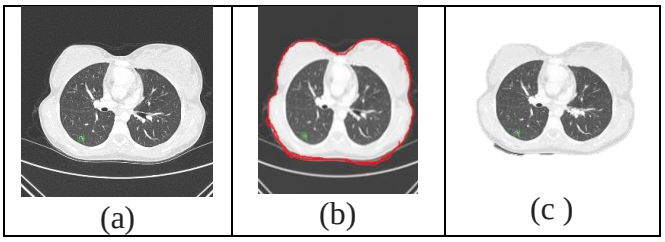

Fig. 3. Steps applied for cropping unnecessary regions from lung cancer CT scans.

C. Data Augmentation

Initially, the dataset of 1142 CT scan segments proved insufficient to effectively train deep CNN architecture. To address this, data augmentation techniques were crucially employed. Six no of different forms of augmentation techniques, such as horizontal flip, rotation, and brightness adjustment, were employed, notably augmenting samples in each class. The innocuous class, initially having the fewest images, underwent the most substantial enrichment. This ensured a more balanced and representative dataset, essential for training the DL model effectively in lung cancer classification. The total amount of CT scan segments for every group prior to and following data augmentation is summarized in Table 4.

Data augmentation technique is exclusively applied to CT scan segments within the training set. Fig. 4 illustrates examples of augmented CT scan segments of lung cancer, showcasing the transformations described earlier. This augmentation technique enhances the diversity and robustness of the training data, crucial for effective deep learning model training.

Table 4 Class wise dataset with and without augmentation

Class	Split-up	No-Augmentation	Augmentation	% per class	Total
Benign	Training	97	1356	33.5	4058
Malignant		450	1356	33.5	
Normal		360	1346	33.0	
Benign	Testing	25			235
Malignant		114			
Normal		96			

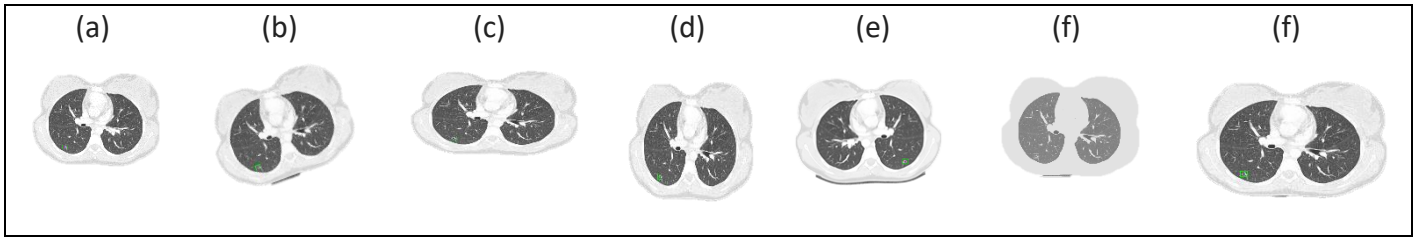

Fig. 4. Original and augmented lung cancer CT scan slices demonstrate the impact of various data augmentation techniques.

Both train and test set images are compressed to 224 × 224 × 3 resolution, aligning with pre-trained EfficientNetB7 model input requirements. This resizing minimizes computation during training while retaining essential image context. Image resizing guarantees input tensor format matches pre-trained EfficientNetB7 models' requirements, reducing computation during training. This process preserves image context, ensuring essential data and characteristics are maintained, thus optimizing model performance while minimizing computational resources. All the three Class labels are encoded as 0, 1, and 2, ensuring consistent representation across sets.

D. Methods

This section goes into discussion on the masked transfer learning methodology and the suggested fine-tuned framework of the EfficientNetB7.

1) TRANSFER LEARNING (TL)

TL is the application of a previously learned model for a new task. Utilizing TL can be trained with a little amount of data has become common in DL. As most real-world issues lack a significant amount of categorized data to train complicated models, it becomes extremely useful in data science. In TL, the generalization of the second task is improved by using what was learned in the first task. By relaxing the requirement, the data can be independent, and generalization can be accomplished [35]. The general architecture of transfer learning is shown in Fig. 5. The elaborate concept is to use the information that the model has learned through performing a novel job with less labelled data. According to how much the information from the previously trained model is applied to the new job, TL may be divided into several methodologies. Five typical TL categories are listed below:

- Feature Extraction: The pre-trained model is utilized in this method as a feature extractor. The output of the remaining layers is used as a feature instead of the final classification layers of the pre-trained model. On top of these collected characteristics, a new classifier is

subsequently trained for your particular assignment. This is especially helpful if you just have a little quantity of data available for the new activity.

- Fine Tuning: In addition to utilizing the characteristics of the previously trained model as a starting point, fine-tuning entails enabling some of the layers to be further trained on the fresh dataset. When the new task and the original task that the pre-trained model was trained on are comparable, this strategy works well. Overfitting must be avoided, though, since too many layers of fine-tuning might cause the model to lose its initial expertise.
- Domain Adaptation: When the target domain (new data for the task) and the source domain (data on which the pre-trained model was trained) are slightly different, domain adaptation is applied. By modifying the model's knowledge to perform well on the target domain, the aim is to close the gap between these domains. There are many methods that may be used, including adversarial training and domain-specific regularization.
- Multitask Learning: A model is trained on several related tasks at once using multi-task learning. The theory behind this is that information acquired from one task might help a person perform better on another one. In this method, the model has levels that are shared by several jobs as well as layers that are exclusive to each activity. When the tasks have certain fundamental characteristics, this can be especially beneficial.
- Zero-Shot Learning: Zero-shot learning is the process of training a model for one task and then applying it to another activity for which it hasn't been given any practise data. Similar to many-shot learning, few-shot learning permits a limited number of instances from the target task during training. These methods can be facilitated by methods like transfer learning using language models (using text descriptions).

The "what to transfer" in learning determines the four settings for the TL process. They include methods for (1) instance transfers, (2) feature transfers, (3) parameter transfers, and (4) relational knowledge transfers [36]. For DL, TL starts with a previously trained stored model.

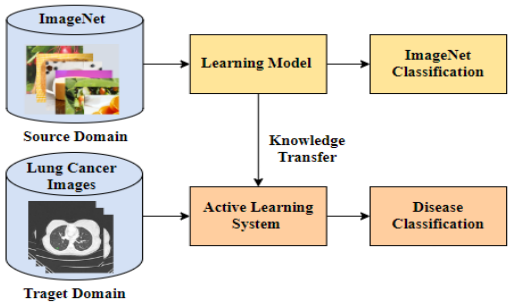

Fig. 5. Architecture of Transfer Learning

This makes it possible to advance quickly and perform well. It is possible to employ a variety of pre-trained CNN models. For image categorization, different models are the designs that were employed in the current study. All categorization studies use input images that are (100x100x3) (100x100x3) in size.

2) MADE, short for Masked Autoencoder for The Distribution Estimation

MADE is a neural network model specifically created to model the probability distribution of data with a large number of dimensions. The MADE variation of auto encoder neural networks was introduced in 2015 by Marc'Aurelio andhis team. It is suitable for applications such as dimensionality reduction, feature learning, and data production. An organized pattern is enforced in the connections between the input and output layers by MADE's use of masks. This pattern guarantees that each output unit depends on only a subset of the input units. Because of this, MADE is able to model complex, high-dimensional probability more efficiently. Density estimation, anomaly detection, and data generation are just a few of the successful applications of MADE in fields as diverse as generative modelling, image modelling, and natural language processing. All things considered, MADE is an excellent tool for understanding data's underlying probability distribution, an essential skill for many statistical modelling and machine learning jobs. The MADE architecture is illustrated in Fig. 6**.**

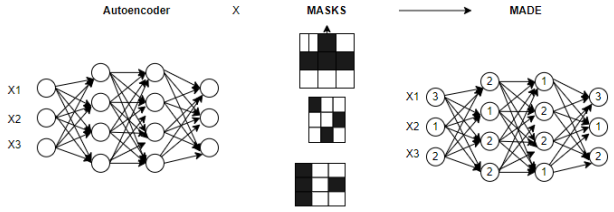

Fig. 6. Architecture of MADE

The MADE algorithm operates by following:

- The structure of an autoencoder, such as MADE, is composed of an encoder and a decoder, similar to a regular autoencoder. Nevertheless, in the MADE model, the encoder and decoder are commonly implemented as neural networks.
- Masking is the primary innovation of MADE. When mapping input data to hidden layers, each hidden unit is independent of the units to its right, given certain conditions. This is achieved by the implementation of meticulously crafted masks that are applied to the weights of the neural network.
- Ordering: In order to guarantee the property of conditional independence, a pre-established sequence is enforced on the input dimensions. Each concealed

unit can only rely on the preceding dimensions in the ordering.

- Training: MADE acquires the parameters of its encoder and decoder networks by maximum likelihood estimation throughout the training process. The goal is to optimize the log-likelihood of the training data based on the model parameters.
- Generation: After being trained, MADE can be utilized to produce samples from the acquired probability distribution by inputting random noise into the decoder.

MADE has demonstrated efficacy in predicting intricate probability distributions, encompassing multimodal and extremely non-linear distributions. It is utilized in diverse fields such as generative modeling, density estimation, and anomaly detection. When it comes to modelling data that has a large number of dimensions and extensive interdependencies, the architecture of MADE is very useful. Through the imposition of conditional independence inside each layer, MADE is able to capture more complicated structures in the data distribution than conventional auto encoders are able to do.

E. Classification using Mask-EffNet:

EfficientNetB7 is a larger model in the EfficientNet family, offering higher accuracy but increased computational resources. It has more layers, wider layers, and operates on higher-resolution inputs. EfficientNetB7 employs compound scaling, a balance between model size and performance, In order to decrease the quantity of parameters and computations while still preserving the ability to convey meaning effectively. In order to reduce the number of parameters and computations that are necessary, EfficientNetB7 makes use of efficient architectural components. These components include squeeze-and-excitation blocks, depthwise separable convolutions, and Swish activation functions. Neural Architecture Search (NAS), which automatically examines the space of alternative designs to find the ones that perform the best, was utilised in order to uncover the architecture of EfficientNetB7. It is possible to use EfficientNetB7 for jobs that need a high level of precision, such as fine-grained picture categorization, medical image analysis, and satellite image analysis; however, this comes at the expense of additional processing resources. EfficientNetB7 architecture comprises a stem block, 7 number of blocks, with a last layer, illustrated in Fig. 7 and Fig. 8.

EfficientNet utilizes even compound scaling for systematical enlargement of the CNN architecture, employing fixed scaling coefficients. This method harmonizes the dimensions of depth (*dh*), width (*wh*), and resolution (*rl*) of the network by scaling them with a consistent ratio, enhancing efficiency and performance. This scaling technique is designed to optimize model performance while ensuring efficient use of computational resources. The mathematical equation for compound scaling is provided in (1) to illustrate this concept.

$$rl = g^{*}phi,\ wh = b^{*}phi,\ dh = a^{*}phi \quad (1)$$

for $a.b^2.g^2 \approx 2$ where, , $g \geq 1$, $b \geq 1$, $a \geq 1$.

The grid search algorithm determines *a*, *b*, and *g* values. *phi*, a user-defined parameter, scales computational resources. Convolutional operation flops relate directly to *dh*, wh^2, and rl^2: doubling network, while doubling width and resolution quadruples flops. Scaling the network via Eq. (1) increases flops by $(a.b^2.g^2)^{*}phi$; each *phi* increment doubles total flops.

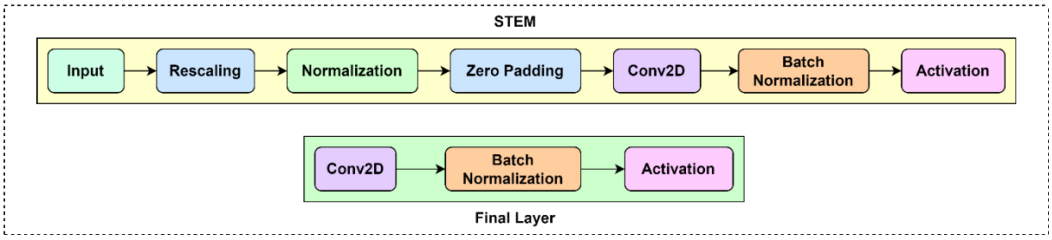

Fig. 7. Stem and final layers of EfficientNetB7

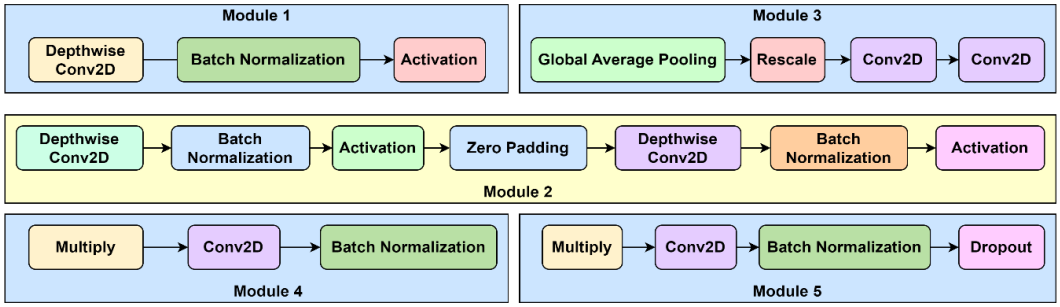

Fig. 8. Modules in EfficientNetB7

4. Proposed Methodology

The study employs transfer learning on a masked EfficientNetB7 variant, utilizing lung cancer CT scan images. Fig. 9 illustrates the masked EfficientNetB7 architecture. Initialization with ImageNet weights primes the base model, enabling fine-tuning of the pre-trained EfficientNet. The Masked Autoencoder for Distribution Estimation (MADE) and EfficientNetB7 are combined for lung cancer classification. This method combines the strengths of both techniques, focusing on data preprocessing, training, feature extraction, and classification head. Data preprocessing involves obtaining a dataset of lung cancer images with annotations indicating the presence or absence of cancerous regions. MADE training is performed on the preprocessed images to learn the underlying distribution of the data, while feature extraction with EfficientNetB7 is used to extract high-level features. Combining MADE and EfficientNetB7 combines the learned representations from both models, capturing both high-level semantic features and fine-grained distribution information. The addition of a classification head, which consists of completely connected layers activated by softmax for binary or multiclass classification, allows for the categorization of lung cancer. With the use of tagged data and a suitable loss function, the model is trained comprehensively. Evaluation and validation are carried out using several evaluation metrics. On top of that, performance is further improved by optimization and fine-tuning. If there is a lack of labelled data, other methods like domain adaptation or transfer learning can be investigated.

To evaluate how well it performs in real-world situations, testing and deployment are carried out on a hidden test set. Prior to deploying the trained model in clinical settings, it must be tested for regulatory compliance and compatibility with the intended deployment environment. Improved accuracy and reliability in identifying malignant regions in lung pictures may result from this methodology's efforts to strengthen the lung cancer classification model's discriminative capacity and resilience.

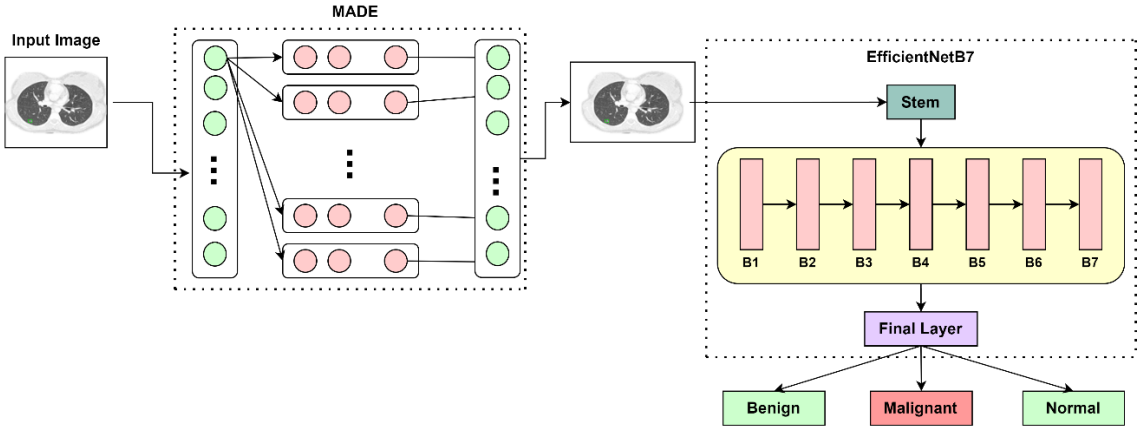

Fig. 9. Proposed Mask-EffNet Model Architecture

5. Results and discussion

The evaluation metrics used to assess the efficacy of the proposed work are discussed in detail in the next subsection. A thorough understanding of the underlying software and hardware is also required before training or evaluating a model. Various matrices are taken into consideration when the proposed approach has been accurately evaluated and implemented. In this part, we also explore the different hyperparameters and the values that go with them. In addition, we present a comprehensive analysis of the data collected using the proposed technique, which sheds light on its efficacy and its consequences. The performance of the technique and its alignment with planned objectives can be better understood with the help of this comprehensive analysis.

A. Performance Metrics

The efficacy of medical image classification into three groups is assessed using the same performance measures as in the previous section specificity through accuracy, sensitivity, and F1 score. To calculate these yield measurements, one uses the following formula:

$$Accuracy = \frac{TN+TP}{TP++FP+TN+FN} \quad (2)$$

$$Specificity = \frac{TN}{FP+TN} \quad (3)$$

$$Sensitivity\ (Recall) = \frac{TP}{FP+TN} \quad (4)$$

$$Precision = \frac{TP}{FP+TP} \quad (5)$$

$$F1\ Score = 2 * \frac{Recall*Precision}{Recall+Precision} \quad (6)$$

In this context, the abbreviations TN, TP, FN, and FP represent True Negative, TruePpositive, False Positive, and True Negative respectively. For the purpose of estimating such parameters, the confusion matrix is utilized. This matrix provides information regarding the incorrect and correct categorization of images across all categories.

- **The ROC Curve:** The receiver operating characteristic (ROC) curve is a graphical representation of the ROC curve's performance at various thresholds. The approach is dependent on two factors, which are the True Positive Rate (TPR) and the False Positive Rate (FPR), which are represented by equations (7) and (8), respectively. The ability of the model to accurately detect true positives while also minimizing the number of false positives over a variety of threshold settings is illustrated by this visualization, which provides useful insights.

$$TPR = \frac{TP}{TP+FN} \quad (7)$$

$$FPR = \frac{FP}{FP+TN} \quad (8)$$

B. Experimental setup.

In order to achieve optimal performance, the mask-EffNet model that has been recommended is constructed using the Google Colab Pro framework. This framework makes it possible to train and evaluate the model more quickly, which is beneficial for the process of developing and testing the strategy that was presented. The experimental configuration employed in this research study is outlined below: This work utilizes Python for model training, explicitly depend on the Keras package with TensorFlow as its backend tool. Utilizing Google Colab pro with T4 GPU which has a substantial 25 GB of RAM that ensures efficient computation and facilitates the execution of complex tasks in machine learning with optimal resource utilization.

C. Hyper-parameters Setup

In order to optimize the training of the model and to get the required results in classifying lung cancer, we performed empirical tests for adjusting several hyperparameters. This include a range of elements such as optimizers and batch size. A decay factor of 0.3 was implemented to enhance learning rate, and drop connect rate of 0.3 was established to provide further regularization during the fine-tuning process, while ensuring that the ImageNet weights remain unaffected. Throughout training, a mini-batch size of 35 was used, with EfficientNetB7 trained for 100 epochs. Validation sets, comprising 20% of training photos per epoch, aided in assessing model efficacy and detecting overfitting. The optimal values for hyperparameters, which were determined after fine-tuning and conducting many test cases which are shown in Table 5.

Table 5 HyperParameters

Hyper Parameters	Values
Input dimension	224 * 224 * 3
Dropping Rate	0.3
Activation Function for output	Softmax
No of Epoch	100
Size of Batch	35
Learning Rate	0.3

D. Analysis of Experimental Results

This study introduces a novel DL approach for lung cancer categorization, employing the Mask-EffNet architecture on CT scan images. The dataset, consisting of 1142 CT scan images sourced from 126 patients, includes 122 benign and 564 malignant cases.

Data augmentation techniques were applied to augment the dataset. The data was split into training and testing sets, maintaining a consistent ratio in both augmented and non-augmented scenarios. This methodology ensures a balanced representation of benign and malignant cases, facilitating robust training and evaluation of the proposed classification model. Prior to being used for training purposes, all of the CT scan pictures underwent pre-processing.

1) Analysis without Data Augmentation

The model that was suggested achieved average test accuracy of 98.36%. Table 6 presents the precise outcomes produced from the Mask-EffNet model with no data augmentation. Fig. 10 displays the graphical representation of the model efficacy in the absence of data augmentation.

Table 6 Performance of Mask-EffNet without data augmentation

Types of Lung Cancer	Recall in (%)	Precision In (%)	F1-Score in (%)	Accuracy in (%)
Benign	93.22	96.47	94.68	98.14
Malignant	99.21	98.18	99.53	98.39
Normal	98.27	97.36	98.45	98.56
Average	**96.90**	**97.33**	**97.53**	**98.36**

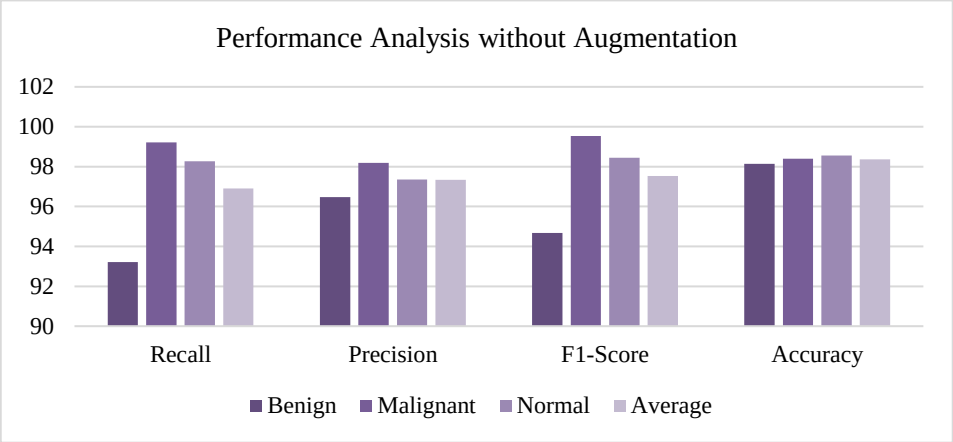

Fig. 10. Performance analysis of the Mask-EffNet without Augmentation of dataset

A confusion matrix is employed to evaluate the ability of a model of categorization to accurately predict outcomes on new, unseen test data. The confusion matrix displays the number of estimated designations on the horizontal x-axis for each class, together with their corresponding true designations on the corresponding vertical y-axis. In this method, the initial step entails comparing the labels predicted by the model with the true labels. Following this, correct predictions are tallied. Fig. 11 displays the proposed approach's performance through a confusion matrix, showing prediction accuracy without data augmentation. This matrix offers a comprehensive breakdown of the model's performance, in terms of classification evaluation.

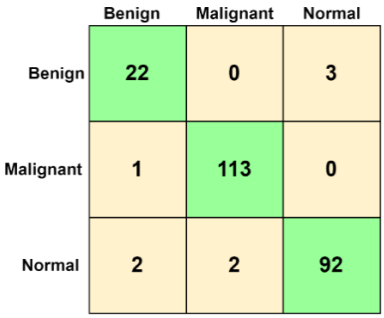

Fig. 11. Confusion matrix without Augmentation

2) Analysis with Data Augmentation

The dataset utilized in the present research incorporated data augmentation and comprised of 4293 lung CT scan pictures sourced from the "IQ-OTH/NCCD dataset".

Among these, 1356 images were classified as benign, 1356 as malignant, and 1346 as normal. Prior to being inputted into the suggested Mask-EffNet model, the photos underwent pre-processing. The model underwent a fine-tuning process using a dedicated training dataset and was subsequently assessed using a separate test dataset. Impressively, it achieved a high test accuracy of 98.98%. The ROC score, ranging from 0.97 to 0.98, further attests to its robust performance. Mask-EffNet models were constructed using a compound scaling technique, ensuring optimal adjustment of depth, width, and resolution while maintaining accuracy and minimizing complexity.

The Table 7 shows the performance of an EfficientNet model with data augmentation for classifying lung cancer into Benign, Malignant, and Normal types. The average metrics indicate strong overall performance, particularly in classifying malignant cases.

Table 7 Performance Analysis of EffNet with data augmentation

Types of Lung Cancer	Recall	Precision	F1-Score	Accuracy
Benign	94.45	96.50	92.96	98.82
Malignant	99.56	98.20	99.29	97.52
Normal	98.88	97.11	95.18	96.40
Average	96.60	96.05	95.03	96.31

With 6 million features, the model demonstrated exceptional performance on the test dataset. Table 8 presents a comprehensive overview of the model's outcomes, including those incorporating data augmentation. Fig. 12 displays the graphical representation of the model efficacy in the with data augmentation. Fig. 13 shows the performance comparison on EffNet without MADE and augmentation versus EffNet with MADE and augmentation. Fig. 14 displays the proposed approach's performance through a confusion matrix, showing prediction accuracy with data augmentation. This matrix offers a comprehensive breakdown of the model's performance, in terms of classification evaluation.

Table 8 Performance Analysis of Mask-EffNet with data augmentation

Types of Lung Cancer	Recall in (%)	Precision In (%)	F1-Score in (%)	Accuracy in (%)
Benign	97.22	99.47	95.65	98.93
Malignant	99.68	99.08	99.53	99.39
Normal	99.25	98.38	98.15	98.63
Average	**98.71**	**98.97**	**97.77**	**98.98**

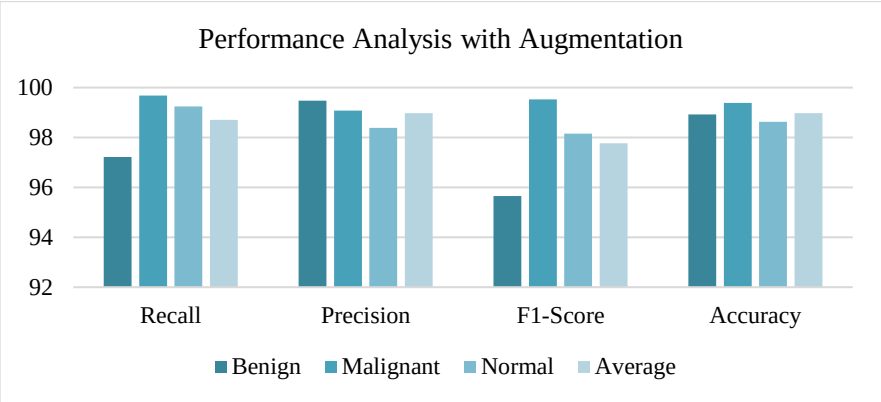

Fig. 12. Performance analysis of the Mask-EffNet with Augmentation of dataset

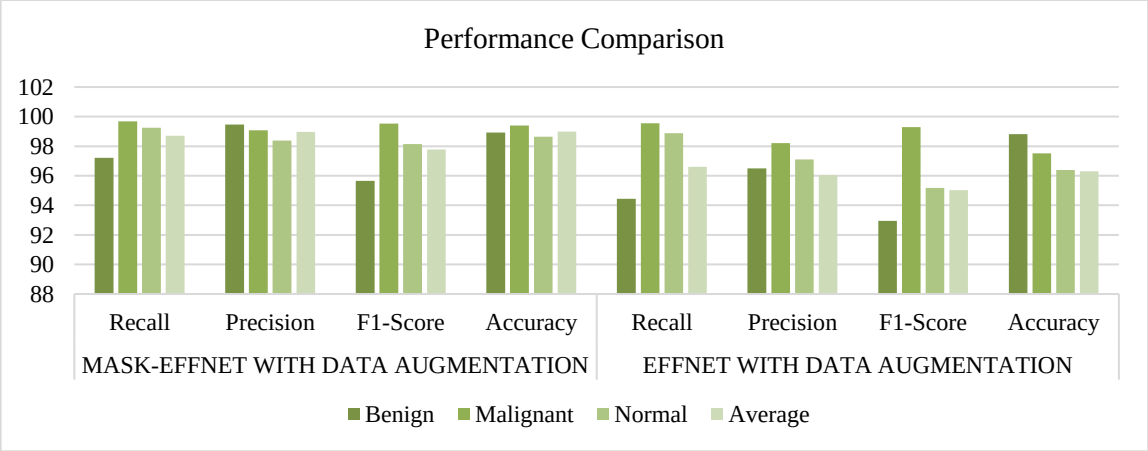

Fig. 13. Performance analysis of the Mask-EffNet and EffNet with Augmentation of dataset

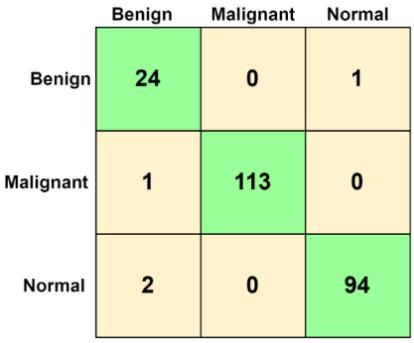

Fig. 14. Confusion matrix with Augmentation

E.Comparison on Lung-EffNet versus previous state-of-the-art methods.

Mask-EffNet has demonstrated improved analysis in the classification of lung cancer operations as compared to other existing models. Mask-EffNet's exceptional performance can be attributed to its capability to extract characteristics from the input photos. Mask-EffNet employs convolutional and pooling layers, progressively extracting image features, enhancing understanding from preceding layers for comprehensive feature representation. This iterative process enables the model to capture intricate visual details critical for precise categorization. Compared with the existing work, the proposed Mask-EffNet architecture has demonstrated superior effectiveness and versatility in image analysis tasks.

The suggested method was evaluated against current models to determine its accuracy. To provide an accurate comparison, the train-test split ratio and dataset were kept consistent. To provide a fair comparison, we will make sure that the ratio of training data to testing data is the same, specifically 80:20. Table 9 contains a detailed examination of the Mask-EffNet protocol compared to the most advanced methods available. The comparison table shows various methods for achieving high accuracy scores in various evaluation metrics. Some methods use CNN, while others use GoogleNet DNN, ShuffleNet with coati optimization, ResNet, MobileNetV2, Xception, VGG16, EfficientNet, and Random Forest. The Mask-EffNet method, which introduces EfficientNetB7 with masked autoencoder, achieves the highest accuracy scores, ranging from 97.77% to 98.98%. Other methods use EfficientNet, GoogleNet DNN, and ShuffleNet with coati optimization. The Mask-EffNet method outperforms others in terms of accuracy with respect to other measure of

matrices. Fig. 15 depicts an extensive performance assessment of the suggested work with current state of the art models.

Table 9 Comparison of different state of the art methods

References	Methodologies	DataSet	Recall in (%)	Precision In (%)	F1-Score in (%)	Accuracy in (%)
Atiya, S [26]	CNN	Own Dataset	97.50	97.78	97.69	97.57
AL-Huseiny [3]	GoogleNet DNN	IQ-OTH/NCCD	97.14	97.14	97.39	98.02
AlGhamdi, R. [18]	ShuffleNet with coati optimization	LC25000	98.39	98.63	97.39	98.88
Shouka et al. [21]	ResNet, MobileNetV2, Xception, and VGG16	IQ-OTH/NCCD	97.46	97.18	96.02	97.69
Raza et al. [14]	EfficientNet	IQ-OTH/NCCD	98.24	98.18	97.61	97.78
Saleh, A. Y. [19]	CNN and Random Forest	IQ-OTH/NCCD	98.19	97.50	96.09	98.79
Chui, K. T. [28]	Modified GAN	NSCLC-Radiomics	97.48	98.16	96.83	95.53
Humayun, M. [27]	VGG16 and CNN	IQ-OTH/NCCD	97.6	97.5	97.25	97.67
Narin N. [7]	AlexNet and ResNet	IQ-OTH/NCCD	98.5	96.8	97.32	98.62
Mask-EffNet (Proposed)	EfficientNetB7 with masked autoencoder	IQ-OTH/NCCD	98.71	98.97	97.77	98.98

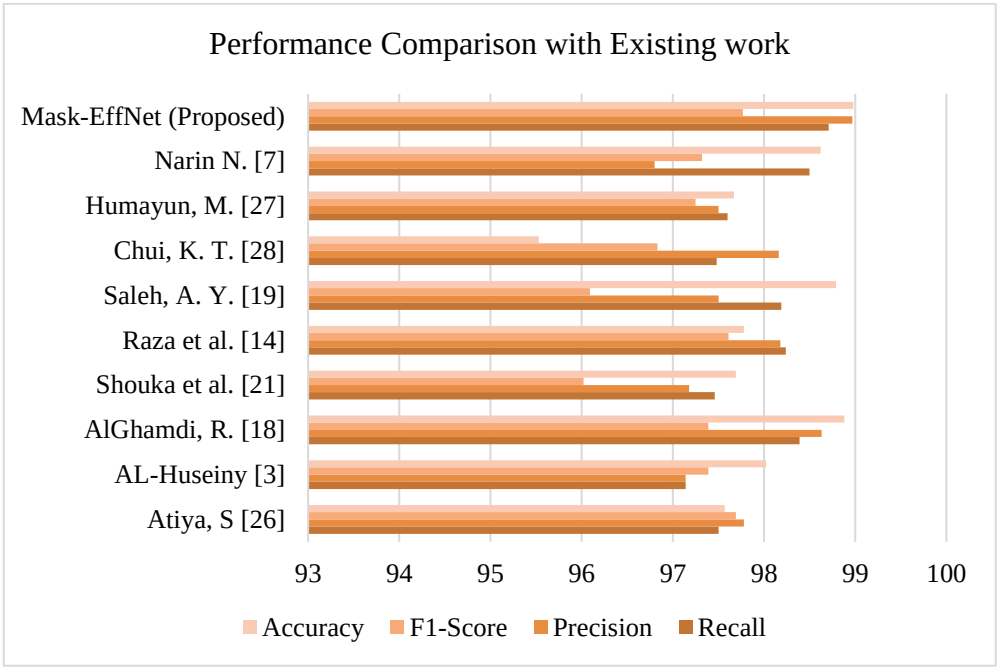

Fig. 15. Performance Analysis comparison of the Mask-EffNet with different existing work

F. The effect of data splitting

Multiple tests are being carried out to investigate the influence of various data divisions on the effectiveness of the suggested Mask-EffNets. To evaluate the model's efficiency, we varied the proportions of training and testing data and thoroughly analyzed the results across different splits. These included the initially suggested 80:20 split, along with 60:40, 70:30 and 90:10 splits, detailed in Table 10. The table presents the results of a model evaluation on different data splits for a classification task. The model achieved recall of 97.23%, precision of 97.43%, F1-Score of 97.99%, and accuracy of 98.19% for the 60:40 data split. For the 70:30 data split, recall was 97.49%, precision of 98.26%, F1-Score of 97.37%, and

accuracy of 98.35%. For the 80:20 data split, recall was 98.71%, precision of 98.97%, F1-Score of 97.77%, and accuracy of 98.98%. For the 90:10 data split, recall was 98.93%, precision of 99.15%, F1-Score of 98.83%, and accuracy of 99.23%. The highest performance was achieved with the 90:10 data split, indicating the model's benefit from more training data. Fig. 16 depicts the efficiency assessment of fine-tuned Mask-EffNets across these splits. Particularly, the model's performance was affected through the partitioned data and emphasizing on the significance of training set size in transfer learning efficiency.

Table 10 Evaluation of Mask-EffNet with different data split-up

Spilt-up	Recall in (%)	Precision In (%)	F1-Score in (%)	Accuracy in (%)
60:40	97.23	97.43	97.99	98.19
70:30	97.49	98.26	97.37	98.35
80:20	98.71	98.97	97.77	98.98
90:10	98.93	99.15	98.83	99.23

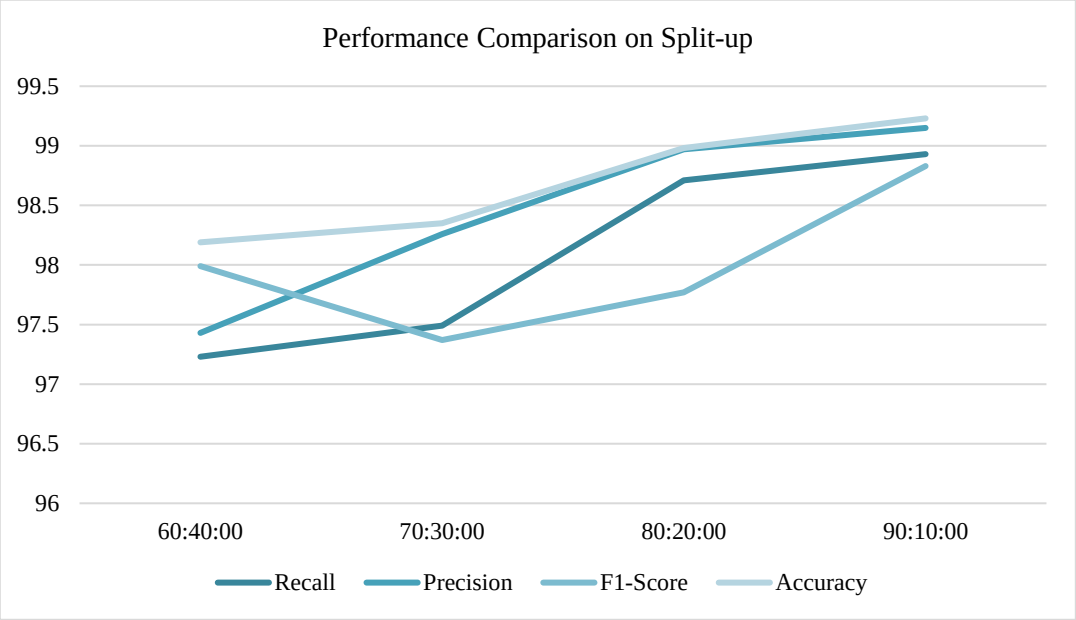

Fig. 16. Performance analysis with various split-ups

G. Computational Complexity

The study meticulously examines the computational complexity of EfficientNet models (B0 to B4), considering parameters, FLOPS, network size, training and inference times, and test accuracy. Following Table 11 the computational profiles of these models alongside other deep learning architectures, all trained and assessed under identical hyper-parameter settings on a shared dataset.

EfficientNetB0 initiates with 4.01 million parameters, progressively expanding in complexity through EfficientNetB1 (6.41 million), B2 (7.60 million), B3 (10.80 million), and B4 (16.65 million). This progression underscores how deeper architectures, characterized by increased convolutional layers, amplify model parameters, thus affecting computational demands in deep neural network design and deployment. Following table show the computational complexity of proposed Mask-EffNet model.

Table 11 Computational Complexity analysis of the proposed Mask_EffNet

Model	FLOPs (G)	No. of parameters	Training time (hh:mm:ss)	Testing time (hh:mm:ss)	Model size (MB)	Test accuracy (%)
EfficientNetB0	0.95	4,021,391	0:03:20	0:00:02	46.2	93.67
EfficientNetB1	1.42	6,417,027	0:46:40	0:00:01	75.4	97.2
EfficientNetB2	1.64	7,605,221	0:50:50	0:00:02	88	96.5
EfficientNetB3	2.38	10,800,843	1:05:20	0:00:02	123.4	97.4
EfficientNetB4	3.71	16,653,995	1:05:50	0:00:04	202.4	96.6
ResNet50	9.13	23,534,592	0:38:02	0:00:03	–	93.5
MobileNet	1.59	3,210,051	0:20:50	0:00:01	36.4	97.8
MobileNetV2	2.72	2,227,715	0:23:20	0:00:01	25.47	97.5
MobileNetV3Small	1.72	928,739	0:00:00	0:00:01	10.56	97.6
Mask-EffNet(Proposed)	15	46,466,851	1:10:50	0:00:07	534.4	98.98

6. Conclusion And Future Work

For the early diagnosis of lung cancer from CT scan pictures, the Mask-EffNet hybrid model, which combines a masked autoencoder for extraction of essential features and a pre-trained EfficientNetB7 for essential classifications, demonstrates promising results. Feature learning, dimensionality reduction, uncertainty estimates, imbalanced data management, transfer learning, and model interpretability are some of the difficulties that are addressed by the model. A ROC score ranging from 0.9782 to 0.9872 degrees and an accuracy of 98.98% were some of the impressive results achieved by Mask-EffNet in trials run on the "IQ-OTH/NCCD" benchmark dataset. These results shed insight on the potential for improving medical imaging diagnostic systems by combining CNN with sophisticated DL techniques.

The benefits of the proposed approach are shown by the experimental results. When compared to other CNN architectures, the Mask-EffNet design always comes out on top in terms of efficiency and accuracy. Moreover, our results have important consequences for future attempts to diagnose and classify lung cancer, particularly using TL in conjunction with EfficientNetB7. New avenues for research and development in medical image analysis are opened up by this method. By demonstrating the efficacy of Mask-EffNet, employing an efficient design model, our work emphasises the possible influence for improved diagnostic accuracy and efficiency in lung cancer detection. These insights provide a foundation for additional research focused on improving and expanding the use of TL techniques in healthcare imaging, finally by contributing to enhanced patient care and outcomes.

A.Future Research

Our findings bear significant implications for lung cancer diagnosis, especially regarding TL with EfficientNets. This approach opens promising avenues for medical image analysis advancement. Future research may explore alternative DL architectures alongside transfer learning, and enhancing model performance through larger datasets and synthetic data generation methods like GANs. Integration of clinical data augments potential research avenues. Expanding datasets to include diverse cases and demographics enhances model robustness. Future exploration of TL with EfficientNets on larger datasets promises deeper insights into model performance across varied scenarios. Augmenting the dataset's size would furnish additional evidence of the efficacy of the proposed methodology in real-world contexts, fortifying its adaptability and applicability across a myriad of clinical scenarios. This comprehensive approach promises to improve the reliability and generalizability of diagnosis of lung cancer disease along with their classification.

REFERENCES

[1] U.S. Department of Health and Human Services, National Institutes of Health, National Cancer Institute, "Cancer treatment," 2023. [Online]. Available: http://www.cancer.gov/about-cancer/treatment.

[2] World Health Organization, "Cancer," 2023. [Online]. Available: http://www.who.int/health-topics/cancer#tab=tab_1.

[3] M. S. Al-Huseiny and A. S. Sajit, "Transfer learning with GoogLeNet for detection of lung cancer," *Indonesian Journal of Electrical Engineering and Computer Science*, vol. 22, pp. 1078–1086, 2021.

[4] Anon, "Chest CT-Scan images Dataset," 2023. [Online]. Available: https://www.kaggle.com/datasets/mohamedhanyyy/chest-ctscan-images. Accessed: June 7, 2023.

[5] Anon, "The IQ-OTH/NCCD lung cancer dataset — Kaggle," 2023. [Online]. Available: https://www.kaggle.com/datasets/hamdallak/the-iqothnccd-lung-cancer-dataset. Accessed: Jan. 19, 2024.

[6] D. B. Krishnamoorthy and S. Padhy, "AI Based Machine Learning Prediction Measure Parkinson Disease Severity," in *International Conference on Machine Intelligence, Tools, and Applications*, Cham: Springer Nature Switzerland, Apr. 2024, pp. 209–219.

[7] D. Narin and T. Ö. Onur, "The effect of hyper parameters on the classification of lung cancer images using deep learning methods," *Erzincan University Journal of Science and Technology*, vol. 15, pp. 258–268, 2022.

[8] N. E. Protonotarios, I. Katsamenis, S. Sykiotis, N. Dikaios, G. A. Kastis, S. N. Chatziioannou, et al., "A few-shot U-net deep learning model for lung cancer lesion segmentation via PET/CT imaging," *Biomedical Physics & Engineering Express*, vol. 8, no. 025019, 2022.

[9] J. Chen, Q. Ma, and W. Wang, "A Lung Cancer Detection System Based on Convolutional Neural Networks and Natural Language Processing," in *2021 2nd International Seminar on Artificial Intelligence, Networking and Information Technology* (AINIT), 2021, pp. 354–359.

[10] H. F. Kareem, M. S. Al-Husieny, F. Y. Mohsen, E. A. Khalil, and Z. S. Hassan, "Evaluation of SVM performance in the detection of lung cancer in marked CT scan dataset," *Indonesian Journal of Electrical Engineering and Computer Science*, vol. 21, p. 1731, 2021.

[11] S. Panigrahy, S. Dash, and S. Padhy, "Predictive Modelling of Diabetes Complications: Insights from Binary Classifier on Chronic Diabetic Mellitus," in *2024 International Conference on Communication, Computer Sciences and Engineering* (IC3SE), May 2024, pp. 1912–1920.

[12] H. Alyasriy and A. Muayed, "The IQ-OTHNCCD lung cancer dataset," *Mendeley Data*, vol. 1, p. 1, 2020. Accessed: Jan. 19, 2023.

[13] N. Kumar, Y. Dash, S. Padhy, S. Dash, and P. Suman, "Improving Breast Cancer Diagnosis: Insights From Machine Learning Models," in *2024 International Conference on Communication, Computer Sciences and Engineering* (IC3SE), May 2024, pp. 1668–1672.

[14] R. Raza, F. Zulfiqar, M. O. Khan, M. Arif, A. Alvi, M. A. Iftikhar, and T. Alam, "Lung-EffNet: Lung cancer classification using EfficientNet from CT-scan images," *Engineering Applications of Artificial Intelligence*, vol. 126, p. 106902, 2023.

[15] A. K. Dubey, G. L. Chabert, A. Carriero, A. Pasche, P. S. Danna, S. Agarwal, et al., "Ensemble deep learning derived from transfer learning for classification of COVID-19 patients on hybrid deep-learning-based lung segmentation: a data augmentation and balancing framework," *Diagnostics*, vol. 13, no. 11, p. 1954, 2023.

[16] O. A. Jassim, M. J. Abed, and Z. H. S. Saied, "Deep Learning Techniques in the Cancer-Related Medical Domain: A Transfer Deep Learning Ensemble Model for Lung Cancer Prediction," *Baghdad Science Journal*, 2023.

[17] R. Wu, C. Liang, Y. Li, X. Shi, J. Zhang, and H. Huang, "Self-supervised transfer learning framework driven by visual attention for benign–malignant lung nodule classification on chest CT," *Expert Systems with Applications*, vol. 215, p. 119339, 2023.

[18] R. AlGhamdi, T. O. Asar, F. Y. Assiri, R. A. Mansouri, and M. Ragab, "Al-Biruni earth radius optimization with transfer learning based histopathological image analysis for lung and colon cancer detection," *Cancers*, vol. 15, no. 13, p. 3300, 2023.

[19] A. Y. Saleh, C. K. Chin, and R. A. Rosdi, "Transfer Learning for Lung Nodules Classification with CNN and Random Forest," *Pertanika Journal of Science & Technology*, vol. 32, no. 1, 2024.

[20] S. Mammeri, M. Amroune, M. Y. Haouam, I. Bendib, and A. Corrêa Silva, "Early detection and diagnosis of lung cancer using YOLO v7, and transfer learning," *Multimedia Tools and Applications*, pp. 1–16, 2023.

[21] T. T. Al-Shouka and K. M. A. Alheeti, "A Transfer Learning for Intelligent Prediction of Lung Cancer Detection," in *2023 Al-Sadiq International Conference on Communication and Information Technology* (AICCIT), Jul. 2023, pp. 54–59.

[22] R. Sharma, S. Kumar, A. Shrivastava, and T. Bhatt, "Optimizing Knowledge Transfer in Sequential Models: Leveraging Residual Connections in Flow Transfer Learning for Lung Cancer Classification," in *Proceedings of the Fourteenth Indian Conference on Computer Vision, Graphics and Image Processing*, Dec. 2023, pp. 1–8.

[23] C. L. Fu, Z. B. Yang, P. Li, K. F. Shan, M. K. Wu, J. P. Xu, ... and F. H. Zhao, "Discrimination of ground-glass nodular lung adenocarcinoma pathological subtypes via transfer learning: A multicenter study," *Cancer Medicine*, vol. 12, no. 18, pp. 18460–18469, 2023.

[24] Z. Ren, Y. Zhang, and S. Wang, "A hybrid framework for lung cancer classification," *Electronics*, vol. 11, no. 10, p. 1614, 2022.

[25] F. C. Laqua, P. Woznicki, T. A. Bley, M. Schöneck, M. Rinneburger, M. Weisthoff, ... and B. Baeßler, "Transfer-learning deep radiomics and hand-crafted radiomics for classifying lymph nodes from contrast-enhanced computed tomography in lung cancer," *Cancers*, vol. 15, no. 10, p. 2850, 2023.

[26] S. U. Atiya, N. V. K. Ramesh, and B. N. K. Reddy, "Classification of non-small cell lung cancers using deep convolutional neural networks," *Multimedia Tools and Applications*, vol. 83, no. 5, pp. 13261–13290, 2024.

[27] M. Humayun, R. Sujatha, S. N. Almuayqil, and N. Z. Jhanjhi, "A transfer learning approach with a convolutional neural network for the classification of lung carcinoma," in *Healthcare*, vol. 10, no. 6, p. 1058, Jun. 2022.

[28] K. T. Chui, B. B. Gupta, R. H. Jhaveri, H. R. Chi, V. Arya, A. Almomani, and A. Nauman, "Multiround transfer learning and modified generative adversarial network for lung cancer detection," *International Journal of Intelligent Systems*, pp. 1–14, 2023.

[29] T. Saikia, R. Kumar, D. Kumar, and K. K. Singh, "An automatic lung nodule classification system based on hybrid transfer learning approach," *SN Computer Science*, vol. 3, no. 4, p. 272, 2022.

[30] S. Nigudgi and C. Bhyri, "Lung cancer CT image classification using hybrid-SVM transfer learning approach," *Soft Computing*, vol. 27, no. 14, pp. 9845–9859, 2023.

[31] S. Dadgar and M. Neshat, "Comparative hybrid deep convolutional learning framework with transfer learning for diagnosis of lung cancer," in *International Conference on Soft Computing and Pattern Recognition*, Cham: Springer Nature Switzerland, Dec. 2022, pp. 296–305.

[32] F. Zhu, R. Zhong, F. Li, C. Li, N. Din, H. Sweidan, ... and Z. Pan, "Development and validation of a deep transfer learning-based multivariable survival model to predict overall survival in lung cancer," *Translational Lung Cancer Research*, vol. 12, no. 3, p. 471, 2023.

[33] S. Wang, L. Dong, X. Wang, and X. Wang, "Classification of pathological types of lung cancer from CT images by deep residual neural networks with transfer learning strategy," *Open Medicine*, vol. 15, no. 1, pp. 190–197, 2020.

[34] R. Patnaik, P. S. Rath, S. Padhy, and S. Dash, "A Novel Optimized Colonic Adenocarcinoma Detection using Deep Transfer Learning Approach with XceptionTS Model," *Journal of Electrical Systems*, vol. 20, no. 7s, pp. 816–830, 2024.

[35] A. B. Dash, S. Dash, and S. Padhy, "Identification of Foxtail Millet Solution for Malignant Colorectal Cell Growth Reduction Using Deep Learning-Based Mobile Net Model," in *The Role of Women in Cultivating Sustainable Societies Through Millets*, IGI Global, 2024, pp. 42–59.

[36] S. Panigrahy, S. Dash, and S. Padhy, "Optimized Deep Belief Networks Based Categorization of Type 2 Diabetes using Tabu Search Optimization," *International Journal of Advanced Computer Science & Applications*, vol. 15, no. 3, 2024.